The International Journal of Advanced Manufacturing Technology
https://doi.org/10.1007/s00170-026-18276-2

ORIGINAL ARTICLE

Mechanical properties of plastic parts produced by molds manufactured by additive manufacturing technology (LPBF) with conformal cooling channels

Alexandre Mateus Popiolek[1] · Louis Laberge Lebel[2] · Carlos Henrique Ahrens[1] · Guilherme Mariz de Oliveira Barra[1] · Adriano Fagali de Souza[1]

Received: 19 February 2026 / Accepted: 1 May 2026

Abstract

Today, additive manufacturing using Laser Powder Bed Fusion (LPBF) allows manufacturing molds of steel containing conformal cooling channels (CCC) to produce plastic parts by injection molding. These cooling channels can improve heat transfer during the molding process, thus reducing the molding cycle time. However, although some studies published in recent years have demonstrated that CCC can enhance productivity, this technology has not been widely adopted by the industries today. There is a lack of information about the mechanical properties of parts produced by molds with CCC, since reducing the molding cycle time can compromise the quality of the parts. Therefore, the current work was conducted to certify the quality of automotive plastic parts produced by injection molding of polypropylene (PP) using a CCC mold manufactured by LPBF. The mechanical properties, microstructure, and dimensional accuracy were assessed and evaluated against the traditional mold (baffle cooling channels - BCC). The results show a reduction of 26% of the molding cycle time using the CCC mold. The higher efficiency on the heat transfer resulted in a reduction of about 47% on the spherulite size and an increase of about 53% of the frozen layer (outer), 6% of the refined layer, and 18% of the skin layer thickness. It resulted in dimensionally more precise parts (83% more precise than the traditional mold). The refinement of the spherulites and the increase in the skin thickness were not enough to alter the results of the impact and tensile test, viscoelasticity, and crystallinity of the parts produced by CCC. Thus, the current work shows that CCC molds can be applied successfully for industrial applications, it can reduce the molding cycle time, improve the parts' accuracy without losing the mechanical properties.

- Conformal cooling cut cycles 26% with higher mass meeting industry criteria.
- Conformal cooling raised frozen, refined, and skin layers 53%, 6%, 18%.
- Uniform heat flow gives 47% lower spherulites, even spread, better nucleation.
- DMA showed stiffness rise with conformal cooling, due to thick skin layer.
- Conformal cooling boosts stiffness, stability at low strain, no strength loss.

Keywords Injection molds · Conformal cooling channels · Mechanical properties · Additive manufacturing

1 Introduction

The mold-making industries play a crucial role as supporting diverse industrial segments, from simple products such as plastic recipients, toys, and medical industries, up to several components of an automobile or an airplane [1]. To achieve a mass production of thermoplastic parts, injection molding is regarded as the most popular manufacturing technology [2]. It enables short product cycles, high-quality surface finishes, and the efficient molding of complex shapes [3].

✉ Alexandre Mateus Popiolek
alexandre.popiolek@posgrad.ufsc.br

1 Universidade Federal de Santa Catarina (UFSC), Florianópolis, Brazil

2 Polytechnique Montréal (POLYMTL), Montreal, Canada

To sustain short product cycles, special attention must be given to the cooling stage, which accounts for more than two-thirds of the molding cycle [4], as it significantly affects the formation of undesired defects such as sink marks, thermal residual stress, warpage, and differential shrinkage [5].

During injection molding, the polymer moves toward the cold mold walls, where it cools and solidifies [6], forming a solid face commonly referred to as skin–core morphology [7]. According to Kantz et al. [8] there are three main layers, to cite: (i) the skin layer, that is often regarded as a thin highly oriented molecular chain, (ii) intermediate layer, also known as the transition zone [9], and (iii) the core layer, that is a region that enables the complete relaxation of chain molecules and the formation of spherulites.

According to Varga et al. [10], the skin layer can vary in three sub-layers, from the surface toward the core, named as: outer, refined, and shear layers. The skin layer influences the material's mechanical behavior [7]. The thickness of the skin layer varies according to resin type and molding conditions. Such variations systematically affect properties like elastic modulus and shrinkage [8].

The part thickness influences the formation and properties of the skin layer. Thicker parts tend to have a more gradual transition between the skin and core layers, while thinner parts exhibit a more pronounced skin layer, as highlighted by Li et al. [11] and Fischer [12]. According to Wright et al. [13], even minor adjustments in processing conditions of semi crystalline polymers can induce substantial morphological changes, however these variations do not translate into significant alterations in the overall degree of crystallinity.

The material of the mold has a significant influence on the mechanical properties of the molded parts [14]. De Souza et al. [15] investigated the morphology of the skin layer and spherulites formed by the injection molding of PP, using different materials to manufacture molds with varying heat transfer properties.

Their findings indicate that higher thermal conductivity in the mold cavity leads to thicker skin layers, smaller spherulites in the core, and reduced cycle time. In contrast, molds with lower thermal conductivity facilitated greater molecular rearrangement, resulting in larger spherulites. The study also examined part deformation, showing that molds made from materials with lower thermal conductivity exhibited a greater tendency toward deformation. According to the authors, this behavior is linked to increased accumulation of residual stress within the thicker core layer of parts produced by these molds.

Therefore, heat transfer in the injection mold affects the microstructure of the molded parts and also influences production time. To improve heat transfer during the injection molding process, cooling channels are manufactured inside the mold cavity to allow cooling fluid to flow.

The traditional manufacturing process for fabricating these cooling channels is drilling, which can produce only linear channels. Then, the technique known as 'baffle cooling channels' (BCC) is commonly used in injection molds, splitting the coolant flow into two semicircular paths inside the mold to enhance heat transfer. Although these channels improve the cooling process, their structural design prevents them from being positioned closer to the part's surface. This limitation weakens their cooling effectiveness, resulting in reduced overall thermal performance [16].

Then, additive manufacturing (AM) of metal parts emerged, enabling the design and manufacture of complex cooling channels that conform to the plastic part's geometry, known as conformal cooling channels (CCC).

The advent of computer-aided processes and the introduction of modern machinery (CAD/CAM - CNC) enable the development of products with free-form shapes, which makes it difficult to conduct heat through the linear cooling channels (BCC) [17]. Thus, the CCC emerges as an important solution to overcome such issues. It may reduce per-piece production costs by increasing the production rate and significantly shortening the cooling time [18].

Xu et al. [19] presented a study on molds using CCC. In this work, the authors explored the design of the CCC, considering the modular design of the cooling channels by dividing the mold geometry into specific regions, and specific channel geometry is designed according to the features of each region. Park and Pham [5] investigated CCC in a spiral, parallel, and zig-zag circuit. The authors concluded that each type of circuit may be more suitable depending on the part´s geometry.

Marques et al. [20] evaluated the design of conformal cooling in terms of the coolant flow circuits' serial and parallel ones. The author concluded that the serial design promoted higher heat transfer because it achieves a turbulent coolant flow, thus resulting in a homogeneous temperature of the mold and lower warpage of the molded part. The work presented by Lu et al. [21] shows a reduction of about 18% on the cycle time using a mold with CCC instead of BCC. Moreover, the residual stresses on the molded parts by CCC were lower than those parts molded with BCC mold.

Using a complex automotive part geometry, Park and Dang [4] showed, by a CAE simulation, a reduction of 35% of the injection molding cycle using a mold with CCC. Extending this simulation work, using the same automotive part, Park et al. [22] achieves a reduction of 23% in a real molding cycle. A little divergence was observed between practical and simulated results, but even that, the CCC achieved a significant reduction in the molding cycle.

The AM technology for metal is still expensive and time-consuming, and in accordance with Singh et al. [23], although the CCC mold is initially more expensive, the total cost per component ultimately becomes competitive. To reduce the AM costs and time, Marin et al. [24] proposed a hybrid manufacturing approach combining machining and AM of metal (Laser Powder Bed Fusion - LPBF) to produce injection mold inserts. In this work, CCC inserts were fabricated with stainless steel powder on pre-machined substrates. This hybrid process reduced the manufacturing costs of the CCC mold by 53%. In this case, the CCC mold reduced cooling time by 36% compared with BCC inserts. The CCC mold produces parts without voids, but the mechanical properties of the plastic parts were not assessed. To certify the mechanical properties of molds produced by hybrid manufacturing, combining machining and AM, Marin et al. [25] showed that this hybrid approach can successfully produce metal parts, reducing LPBF cycle times and costs and ensuring mechanical properties.

In addition to hybrid manufacturing and other approaches to reducing AM time and costs, the natural technological development leads to a reduction in the costs of the AM process itself. This indicates that an increase in the use of molds with CCC is expected, unless the quality of plastic parts produced by these molds is not guaranteed.

Based on the literature reviewed to date, the design of CCC, the manufacture of metal AM molds for CCC, and the reduction of the injection cycle using CCC molds are documented. However, there is a lack of publicly available data on the properties of plastic parts produced by CCC molds.

For industrial applications, it is essential to understand that the cycle time reduction enabled by the CCC molds does not affect the quality of the molded parts.

Therefore, the current work was conducted to certify the quality of plastic parts produced by injection molding of polypropylene (PP) using a CCC mold manufactured by LPBF. Using an automotive component as a workpiece, a set of experimental injection molding batches was conducted. After that, in addition to the molding cycle time and geometric form errors, the microstructure and mechanical performance of the parts were assessed.

2 Experimental procedure

To achieve the aims of this work, two molds with different cooling channels were designed and manufactured: (i) a mold manufactured using additive manufacturing of metals (LPBF) with conformal cooling channels, and (ii) a conventional counterpart mold manufactured using traditional machining, containing linear cooling channels (baffle design). Both molds produce the same automotive component.

The molding cycle time was assessed, as well as the geometric form errors of the produced parts. Then, the plastic parts were characterized by tensile tests, deformation energy absorption, degree of crystallinity, and viscosity. To have a better comprehension of the molding phenomena using both different cooling systems of the molds, MEV and POM images were obtained to investigate the skin/core thickness and the spherulite size and its distributions. The overall experimental workflow is summarized in Fig. 1, with methodological details described in subsequent sections.

2.1 Workpiece geometry and mold set-up

Figure 2a shows the workpiece (automotive plastic component). It was chosen because it is an accurate assembly component that requires high accuracy. Figure 2b shows the injection mold with its main parts and the conception of the interchangeable inserts: (i) conformal cooling inserts and (ii) baffle inserts. Figure 2ci shows the baffle cooling channels of the conventional insert manufactured by machining of PH13-8Mo stainless steel and Fig. 2cii shows the conformal cooling channels of the insert manufactured by LPBF, using a 400 W YAG fiber laser machine (CL50WS, Concept Laser) with a spot size of 100 μm and a wavelength of 1064–1070 nm, using stainless steel powder with C 0.03%, Cr 12%, and Ni 9.2% (Corrax).

The plastic workpiece was designed to weigh 34.5 g. A simple analysis of mass was conducted using a digital weight.

2.2 Injection molding experiments

The plastic parts were produced in two batches of 15 parts each, using virgin homopolymer polypropylene (PP, H301, Braskem). The first batch used the BCC, and the second used the mold with CCC. To evaluate the parts produced under a constant molding regime, the first 10 parts of each batch were discarded, leaving only 5 parts for evaluation. Table 1 shows the injection molding parameters set on the injection machine Primax R100, Romi S.A.

For both molds, the cooling time was set during a try-out phase, starting with a common rule of thumb that the cooling time is influenced by the square of the thickest wall of the part and the largest runner diameter raised to the exponent 1.6 [26]. According to Marques et al. [20] it is expressed as:

$$T_c \infty \left(Th_w^2 + D_r^{1.6}\right) \tag{1}$$

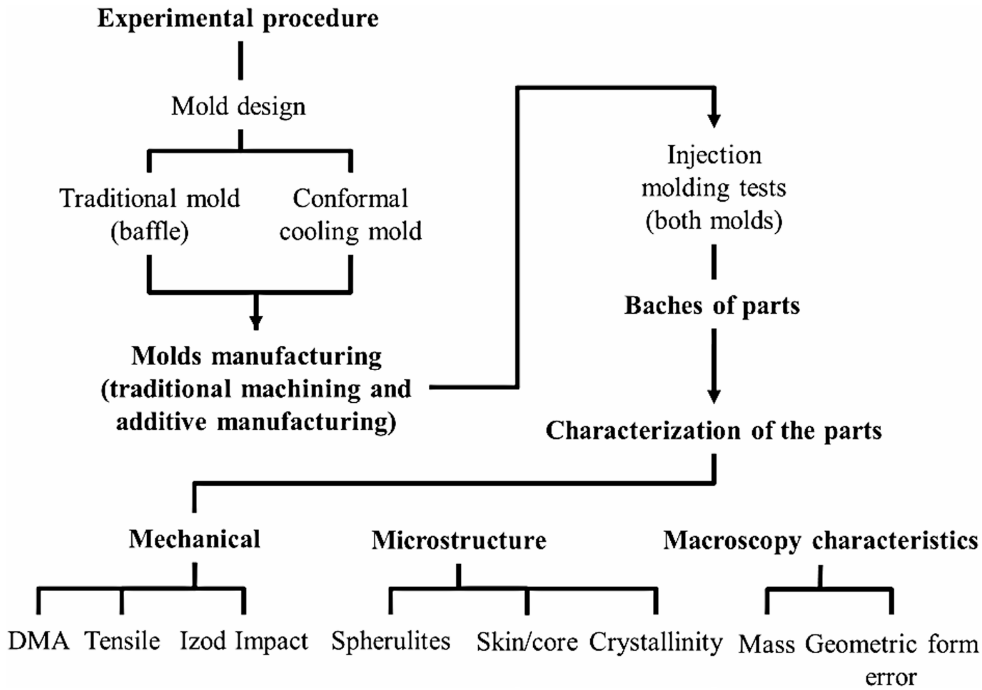

Fig. 1 Flow chart of the experimental procedure

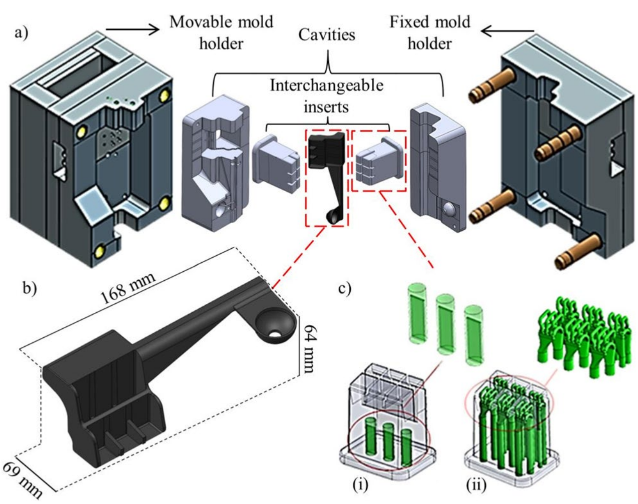

Fig. 2 Mold set-up (**a**), workpiece geometry (**b**), and cooling channels (**c**) for baffle ordinary drilled (i) and conformal cooling additive manufactured with metal (ii)

Table 1 Injection parameters

Parameter	Values	
	BCC	CCC
Injection pressure (bar)	550	
Counter pressure (bar)	12	
Cooling time (seconds)	23	17
Injection temperature (°C)	240	
Dosage (cm^3)	72	
Holding pressure (bar)	10	
Water flow (l/min)	6	

where T_c is the cooling time in seconds, Th_w is the thickness at the thickest part wall (mm) and Dr is the diameter of the largest runner (mm).

The thickest region of the part is 3.51 mm, and the bigger diameter of the runner is 5.40 mm. By applying Eq. (1), the resulting value for Tc was 27 s. Both the BCC and CCC inserts started with the same cycle time, which decreased in increments of 2 s after every 10 cycles, until good parts could no longer be extracted using the automatic cycle. From Table 1, it is possible to observe that good parts were extracted from BCC up to a cooling time of 23 s, while for CCC, this value decreased to 17 s (saving about 26% of the injection cycle).

Immediately after removal from the mold, the workpieces were separated from the runners and cooled at room temperature, placed on a table of low thermal conductivity. For the measurement, it was awaited 48 h after the parts had been removed from the mold, according to the standard ASTM D955:21.

2.3 Evaluation of the geometric form error

The geometric form errors of the molded workpieces were evaluated by a coordinate measuring machine (model Legex 9106, Mitutoyo). Surface measurements were conducted with a touch probe that recorded three data points per surface of interest, enabling a comparison with the corresponding CAD 3D. The form deviation (FD) can be determined by [19]:

$$FD = D_m - D_0 \tag{2}$$

where D_0 is the original dimension, D_m is a measured dimension, with no deviation when a value of zero is presented. Figure 3 displays a sectional view of the positions of the three measurement points on each surface for reference.

2.4 Mechanical characterization: impact, tensile, and viscoelasticity

Figure 4 presents the regions from which the samples for mechanical tests were extracted from plastic workpieces. For DSC analyses, samples were extracted from the top, middle, and bottom regions (samples 1, 5, and 6). These samples were extracted from workpieces to characterize the plastic parts produced by both molds under evaluation, conformal cooling, and baffle.

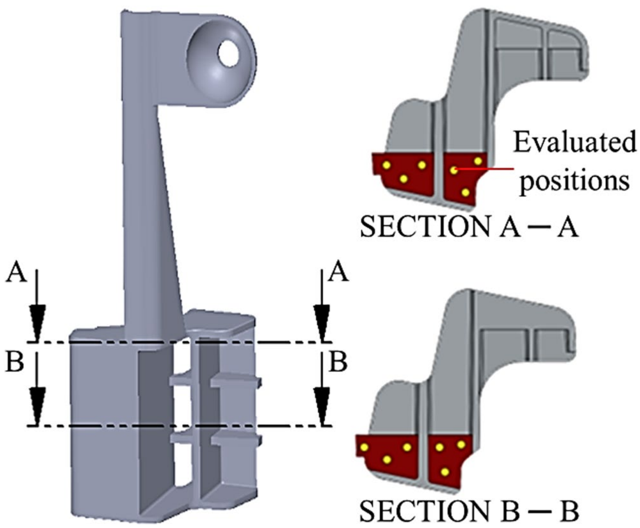

Fig. 3 Regions of measurement of geometric form errors

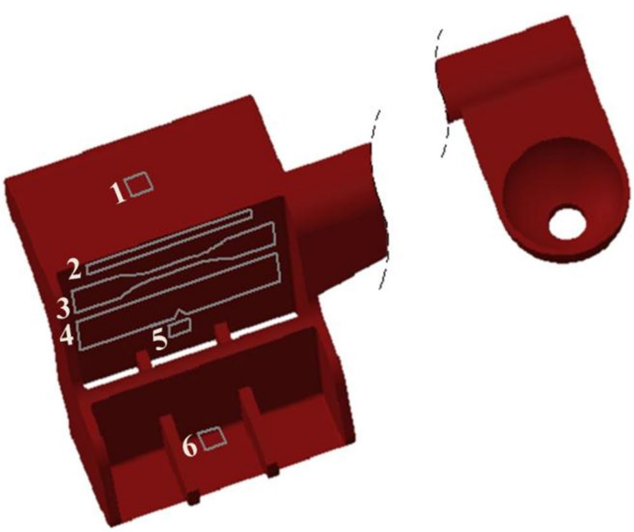

Fig. 4 Regions where the samples were extracted for DSC (1, 5, and 6 - top, middle, and bottom regions), DMA (2), impact (4), and tensile tests (3)

The impact tests were conducted in an Izod Impact device for plastics (EMIC model AIC-1, Instron), using the Izod method according to ASTM D256/2023 standard (ASTM, 2023) and a 2.70 J pendulum, with the effective length of 327 mm, impact speed of 3.45 m/s, fall height of 610 ± 2 mm and fall angle of 60° from the horizontal, according to machine procedure [27].

The tensile test was performed using a universal testing machine (EMIC model 23–100, Instron) equipped with a high-precision 5 kN load cell. The test was conducted at a constant speed of 5 mm/min in accordance with ASTM D638/2014.

Digital Image Correlation (Q400, Dantec Dynamics, Inc.) was utilized to measure displacements via a point-tracking algorithm, with an acquisition rate of 200 ms (5 Hz), synchronized with the tensile testing machine. Additionally, individual video frames were exported and analyzed using image strain analysis software (Instra 4D, Dantec Dynamics, Inc.), enabling visualization of the strain field as a continuous spatial variable.

The viscoelastic performance of the materials was carried out in a DMA machine (242 E Artemis, Netzsch), according to ASTM D4065 (2020) programmed with traction mode with a force of 4 N, amplitude of 25 µm, temperature between − 50 °C and 120 °C, and the frequency was constant at 1 Hz. The samples were prepared according to ASTM D256 and ASTM D638 standards. Due to their complex shapes and dimensional requirements, they were stamped using a press-forming apparatus.

2.5 Degree of crystallinity

The crystallinity was analyzed across samples extracted from the workpiece, considering three critical regions (in terms of heat): the top, middle, and bottom surfaces of the core region of the workpiece, as presented in Fig. 4. Besides, a reference region, in a non-critical area of the workpiece, was included to evaluate the crystallinity. The samples were fit inside the aluminum hermetically sealed pan, which has a volume of approximately 20 µL. A Q Series™ 2000 machine from TA instruments© was used with nitrogen as a purge gas with a volume flow rate of 50 ml/min, 2 cycles (heat, cool, heat), initial temperature set to room temperature, final temperature of 210 °C, heat rating of 10 °C/min, and cooling temperature of -90 °C.

2.6 Skin and core thickness and analysis of the spherulites

The thickness of the skin and core of the cross-section of the molded parts was examined. The cross-section samples were extracted by cryogenically fracturing, as illustrated by Fig. 5. After the fracture, the samples were coated with a 10 nm layer of chromium to be better analyzed by a scanning electron microscopy (SEM) (model TM3030 Plus, Hitachi High-Tech Corporation). The specimens were 17 mm x 15 mm with a 2 mm thickness.

The same samples as Fig. 5 were used to slice thin films to analyze the spherulites' morphology, using a POM.

Thin films of 5 µm were cut from the top of the sample, with a total width of 2 mm, in the flow thickness plane. The films were cut by a cryostat microtome (CM1850; Leica Microsystems, Inc.) equilibrated at -35 °C for 30 min, equipped with a disposable stainless-steel razor with a high-profile blade. The specimens were sliced by 20 µm until no imperfections of the cryofracture were observed to obtain the film to be evaluated.

The films were fixed on the cryostat table with optimal cutting temperature compound (Tissue-Tek, Sakura Finetek), embedded in a common blister pack that better accommodates the size of the sample. To mount the films on the slides for imaging, double-distilled vegetable glycerin was used. To preserve the films, the edges of the coverslip were sealed with colorless varnish.

The images of the spherulitic growth morphology were captured using a polarized optical microscope POM (OLYMPUS BX50, Olympus Co.) coupled with a 5.0 MP color digital camera with standard C-mount CMOS sensor (SLMI 093, Opton) and the ISCapture software (Version 3.7.8.2, Xintu Photonics Co.), equipped with a Plan Achromat lens. The images were captured for the workpieces produced by both molds, BCC, and CCC.

Additionally, the mass of five workpieces produced by both molds was measured using a semi-analytical balance (Model Sartorius CPA1245) with a sensitivity of 0.3 mg.

3 Results and discussions

From a productivity point of view, a reduction of 26% on the cooling time was achieved using the mold with conformal cooling channels, as presented in Table 1. A reduction in the cooling time was expected because the CCC promotes higher heat transfer.

Considering the geometric form error, the four positions at the workpiece checked by the CMM (presented in Fig. 3, A to D), together to its nominal dimensions (3D CAD): A = 39.28 mm, B = 38.68 mm, C = 20.18 mm, D = 20.10 mm, were used in Eq. (2) to identify the form error (mm). Five workpieces produced by each mold (CCC and BCC) were evaluated to have statistical confidence.

Figure 6 illustrates the form deviation, as well as the statistical difference between BCC and CCC inserts parts, where it is possible to observe that the difference between BCC and CCC is significant on all surfaces.

Figure 6 highlights the accuracy of the workpieces achieved by the CCC molds, which propitiate the highest deviation of about 0.3 mm, whereas for the parts produced by the conventional mold (BCC), the lowest deviation was about 0.8 mm, and the highest was about 1.3 mm. In addition to the fast cooling rates, the CCC also produces more precise parts, likely due to more homogeneous heat transfer.

3.1 Mechanical characterization

Figure 7a exhibits the average energy absorbed by the parts produced by the BCC mold, which was about 19 J/m (standard deviation of 5.3), whereas the parts produced by the CCC mold were 21 J/m (standard deviation of 9.3). The average values of stress-strain curves obtained from 5 samples extracted from each workpiece produced by BCC and CCC are presented in Fig. 7b.

It was not possible to identify divergences in the energy absorbed by the parts produced by the BCC mold and the parts produced by the CCC. But, to have statistical confidence, the Shapiro-Wilk test was applied. It was observed

Fig. 5 Process of SEM sample extraction through cryofracture

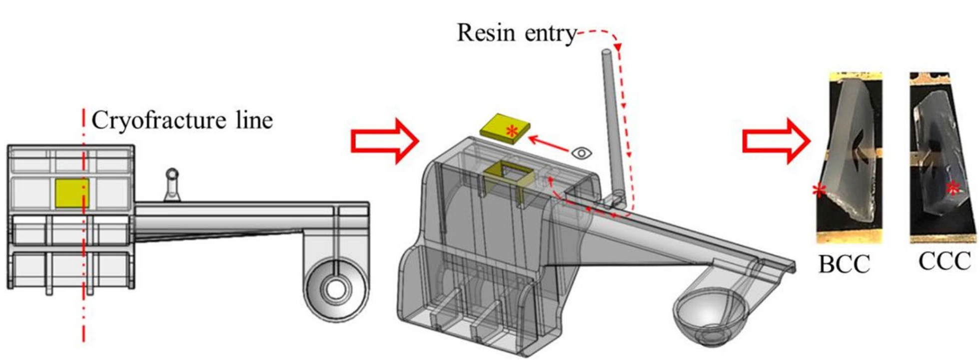

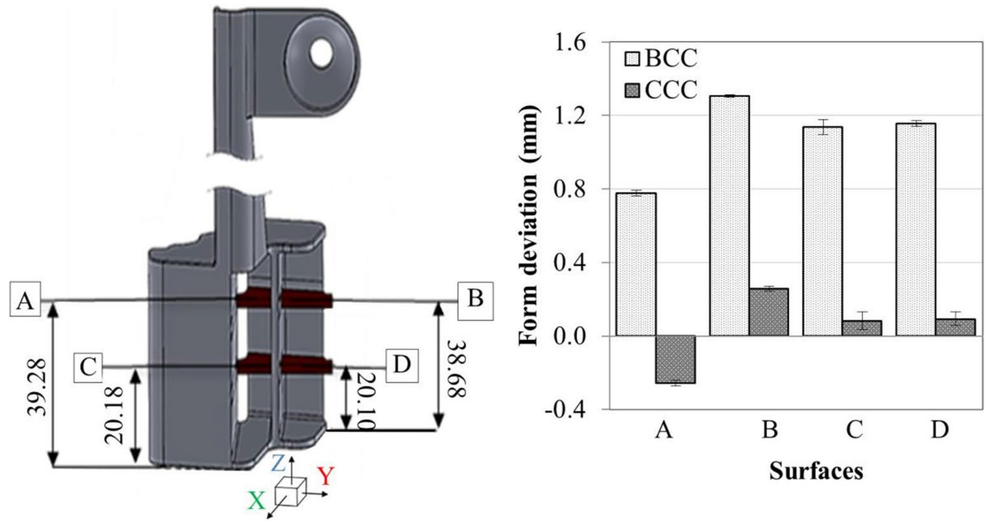

Fig. 6 Geometric form error observed in the workpieces produced by both molds (CCC and BCC)

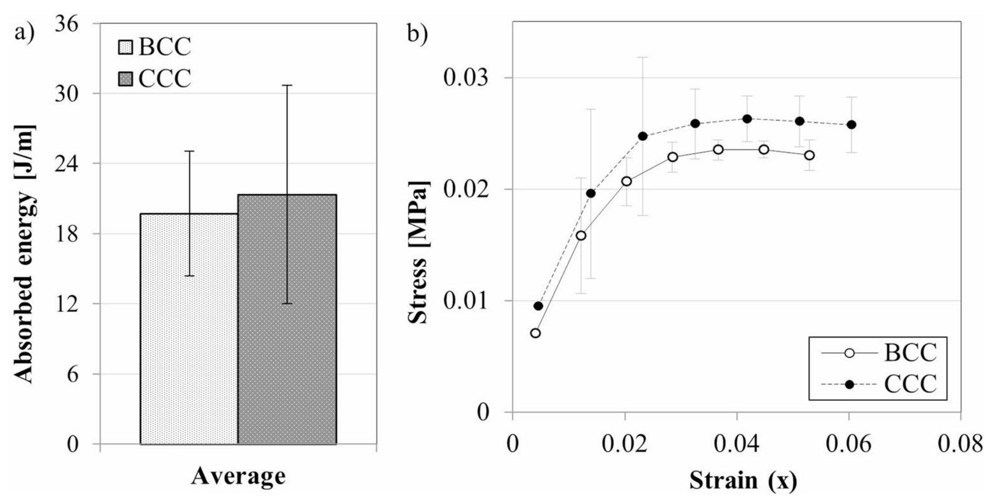

Fig. 7 Absorbed energy from impact testing (**a**) and average stress–strain curve for BCC and CCC samples (**b**)

that CCC follows a normal distribution, W $(5)=0.96$, $p=0.81$, while BCC does not, W $(5)=0.73$, $p=0.02$. The Mann-Whitney U test for two independent samples indicated no statistically significant difference in impact resistance values between BCC and CCC ($W=10.5$, $p=0.75$).

The Shapiro-Wilk was also applied to understand the tensile tests. Results indicates that BCC (W $(7)=0.74$, $p=1.04\times10^{-2}$) and CCC (W $(7)=0.69$, $p=2.55\times10^{-3}$) data suggests a non-normal distribution. The Mann-Whitney U test for two independent samples indicated no statistically significant difference in impact resistance values between BCC and CCC ($W=11$, $p=0.097$).

For the Shapiro–Wilk test, the null hypothesis (H_0) states that the data follow a normal distribution, while the alternative hypothesis (H_1) states that the data do not follow a normal distribution. For the Mann–Whitney U test, H_0 states that the distributions of the two groups are equal, while H_1 states that they differ. Statistical significance was evaluated at the 0.05 level, such that results with $p\leq0.05$ were considered evidence against H_0.

Therefore, based on the tensile and impact tests, no statistically significant divergences were found between parts produced by CCC and BCC molds. Then, to identify possible alterations on parts produced with lower cooling time by the CCC mold, the next analyses were completed.

3.1.1 Degree of Crystallinity

In Fig. 8 (*a-c*) the DSC curves of parts produced by BCC and CCC molds are presented, considering three regions of the workpiece: top, middle, and bottom. It shows the values of the enthalpy of crystallization $\Delta H_f\,(T_c)$ in J/g and the temperature at the melting point Tc in ºC of each one.

It is interesting to note that DSC curves of parts produced by BCC and CCC molds had little divergence according to the region evaluated. At the top region (Fig. 8a), the curves had a little divergence because, even though the CCC acts in this region, the material is at an elevated temperature since it is near the entrance gate. In the middle region (Fig. 8b), the cooling channels are linear for both, which

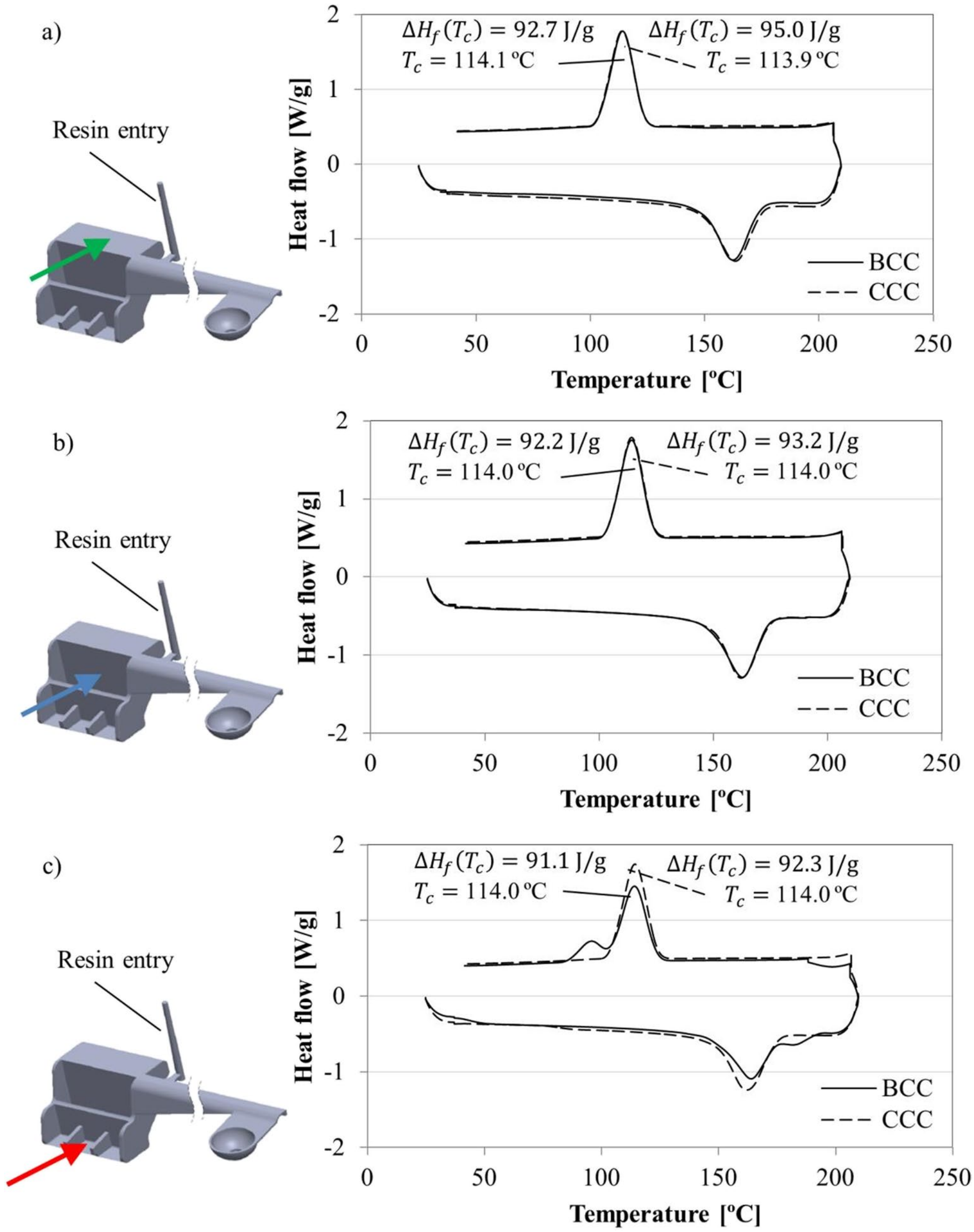

Fig. 8 Contrast between BCC and CCC inserts: top (**a**), middle (**b**), and bottom (**c**) regions of the workpiece

means a similar molding condition, thus the curves are one over the other.

At the bottom (Fig. 8c), the CCC acts, but the material at this point is colder than the top region. Probably, this is the reason for the little divergences on the DSC curves. Such a difference was not sufficient to alter the mechanical properties of the impact and tensile tests. The crystallization melting peak was calculated using the values presented in Supplementary Material [28].

Figure 9 presents the average degree of crystallinity (Xc_Tc) in % for the plastic parts produced by BCC and CCC molds, of the three regions evaluated (bottom, middle, and top).

Figure 9 show that the reduction of the cooling time propagated by the CCC mold did not alter the crystallinity degree of the parts. It is more related to the material properties than the processing conditions.

3.1.2 Dynamic mechanical analysis (DMA)

Figure 10 (*a-b*) presents the results of the DMA analyses for BCC and CCC samples. Figure 10a shows the storage modulus (E′) behavior, where the glass transition temperature (Tg) can be identified from the onset of the modulus drop. In both inserts, a decrease in E′ is observed around − 16 °C, which corresponds to the E′-based Tg. Figure 10b illustrates the tan δ curves, from which the primary Tg is determined more precisely. For both BCC and CCC, the tan δ peak appears at approximately 10 °C, confirming that Tg

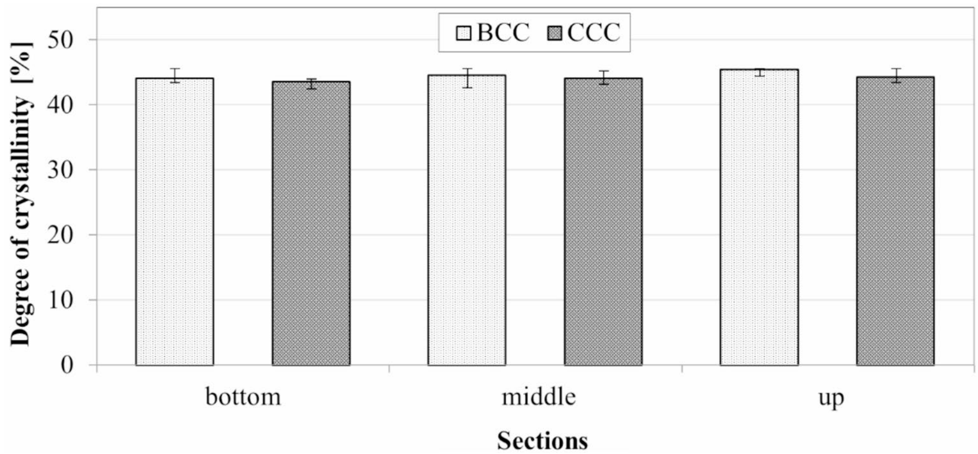

Fig. 9 Bottom, middle, and top areas average values of degree of crystallinity for BCC and CCC inserts samples contrasted with the reference value

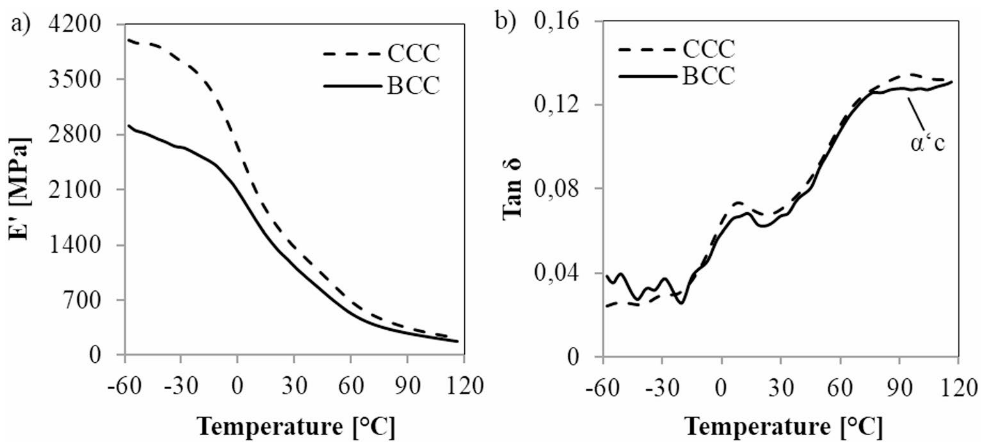

Fig. 10 Relaxations from the DMA test sectioned in E' modulus (**a**) and tan δ (**b**), for BCC and CCC samples

is an intrinsic property of the polypropylene backbone and remains consistent across grades of the same polymer [29]. In addition to the main transition, Fig. 10b also reveals the presence of the α′c secondary relaxation around 85 °C for both BCC and CCC samples.

The normality of the data was assessed by Shapiro-Wilk test for E' ($p = 2.44 \times 10^{-08}$ and $p = 1.24 \times 10^{-08}$) and tan δ ($p = 7.06 \times 10^{-08}$ and $p = 1.18 \times 10^{-07}$), which showed that all distributions were non-normal for BCC and CCC respectively. Consequently, the Mann-Whitney U test was employed, resulting in $p = 1.36 \times 10^{-02}$ and $p = 0.50$ for E' and tan δ respectively. In addition, for E', CCC shows a higher median value (around 1400) compared to the BCC group (around 1100). Regarding tan δ, both BCC and CCC have equal median values (0.07). The interquartile range (IQR) of CCC also appears larger (2867.83 MPa for E' and 0.09 for tan δ), compared to BCC (2077.55 MPa for E' and 0.08 for tan δ), indicating greater variability in the data.

It can be inferred that the observed difference between E' of the samples produced by both molds is statistically significant. However, for tan δ, the null hypothesis is accepted, indicating no significant difference between the BCC and CCC groups. Hence, CCC exhibits a higher storage modulus, indicating slightly increased stiffness.

3.2 Skin and core layers and spherulites morphology

The analysis of mechanical properties in macroscale (impact, tensile, and crystallinity) did not show a difference among the parts manufactured by both molds (CCC and BCC). However, the DMA showed that the parts molded by CCC had a higher storage modulus (E′) than those molded by the BCC mold. To understand that result, the skin and core thickness as well as the spherulites morphology were assessed.

Then, the skin-core layers and the spherulites morphology were investigated by SEM and POM images, respectively, as presented in Fig. 11 (*a-d*). It shows the skin-core layers of one sample of BCC (Fig. 11a) and one sample of CCC (Fig. 11b), which were examined using a cryofracture section of the area in contact with the inserts, with observations made on the fractured surface. The samples were coated with a 10 nm layer of chromium. Figure 11c and d

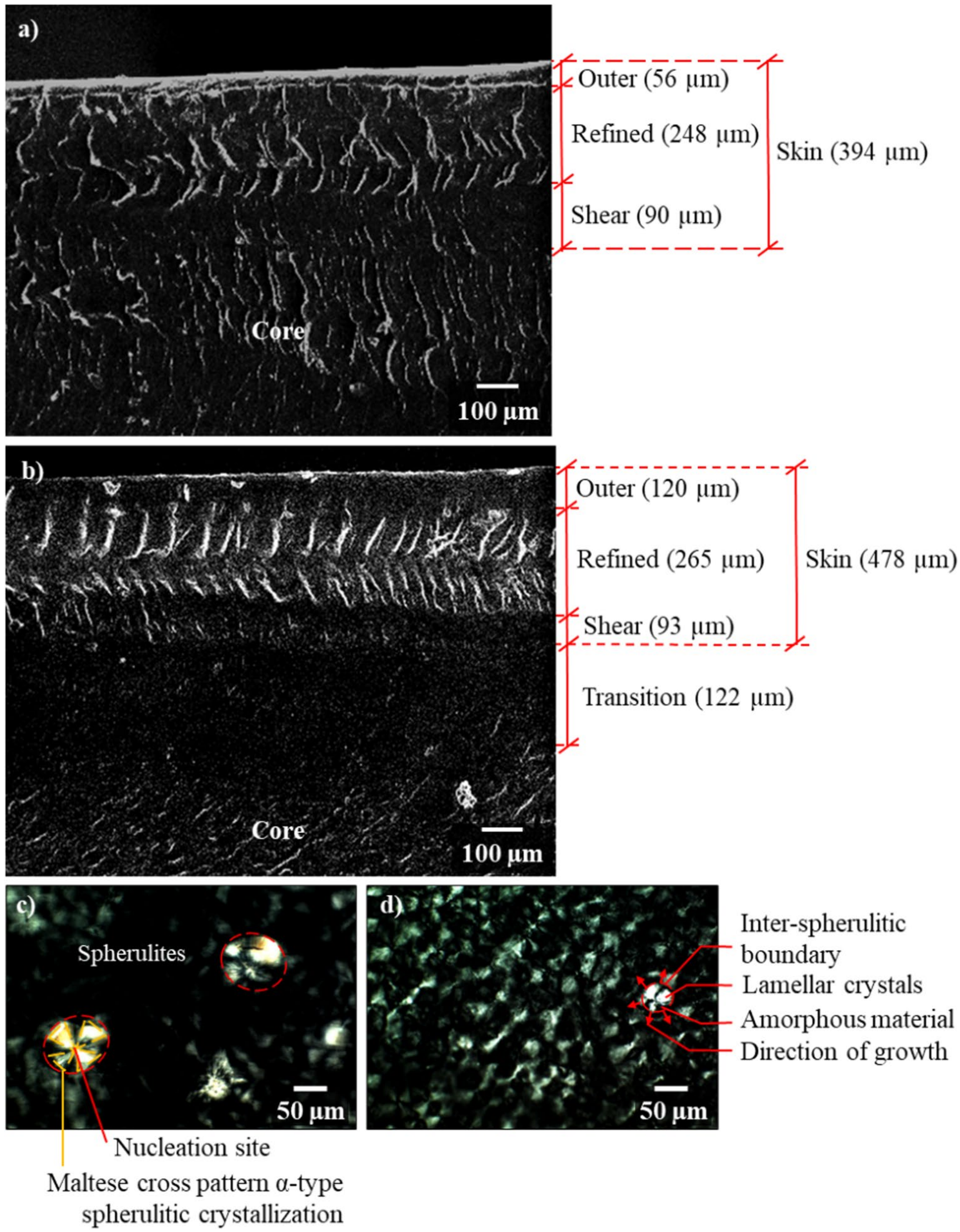

Fig. 11 SEM images with 80x magnification across the length of the cross section of the cryo-fractured samples of the injected parts layers (**a, b**) using BCC and CCC molds respectively and POM images of the core layer captured under crossed polarized light (**c, d**) for BCC and CCC molds, respectively

exhibit samples of micrographs of the core layer from BCC and CCC molds, respectively.

Observing the Fig. 11b it is possible to observe an extra layer called transition which according to de Souza et al. [15] occurs between the core and the shear zone, and as states Zhu et al. [30] it works as a bridge transmitting tensions from one phase to another, meaning that if more pronounced the transition layer bigger the chances of adhesion between the phases. In the CCC mold, the cooling system provides a more uniform heat extraction, which leads to a smoother decrease in molecular orientation from the shear layer toward the core. For Fig. 11a and b, this comportment is not evidenced as higher mold temperatures reduce the viscosity, allowing the material to flow more smoothly. Table 2 summarizes the thickness of the skin and its sub-layers and the core layer for BCC and CCC samples.

From Table 2; Fig. 11b, it is possible to observe that, with a high cooling rate, a quick solidification of the outer skin layer occurs, leaving the core molten longer,

Table 2 Skin to core layers thickness for BCC and CCC

Cooling Channel	Skin sub-layers			Skin [µm]	Tran-sition [µm]
	Outer [µm]	Refined [µm]	Shear [µm]		
BCC	56	248	90	394	-
CCC	120	265	93	478	400

resulting in a thicker skin. Conversely, a low cooling rate allows slower solidification and crystallization throughout, leading to thinner skin.

Besides the skin/core thickness, the morphology of the spherulites was evaluated by images from a POM. Figure 11 (*c-d*) displays the cluster of spherulites, with random orientation relative to the plane, exhibiting variations in density and magnitude of crystalline structures.

For the parts produced by the BCC molds, the spherulite distribution within the core layer was sparser, and the spherulites formed during solidification were larger (Fig. 11c) compared to the ones observed on the parts produced by the CCC mold (Fig. 11d). This indicates that the cooling strategy plays a critical role in the crystallization behavior of polypropylene, with traditional cooling promoting fewer but larger spherulites, likely due to slower and less uniform heat dissipation during solidification.

3.3 Mass of the parts molded by BCC and CCC molds

Figure 12 shows the average and standard deviation of the mass of the molded workpieces. It indicated that pieces produced by the CCC mold averaged 34.2 g, whereas those produced by the BCC mold averaged 33.9 g, with the workpiece designed to weigh 34.5 g. The mass for the evaluated samples from the BCC and CCC follows a normal distribution (H_0), as assessed by the Shapiro–Wilk test. The t-test indicated a statistically significant difference (H1) between the means of BCC and CCC.

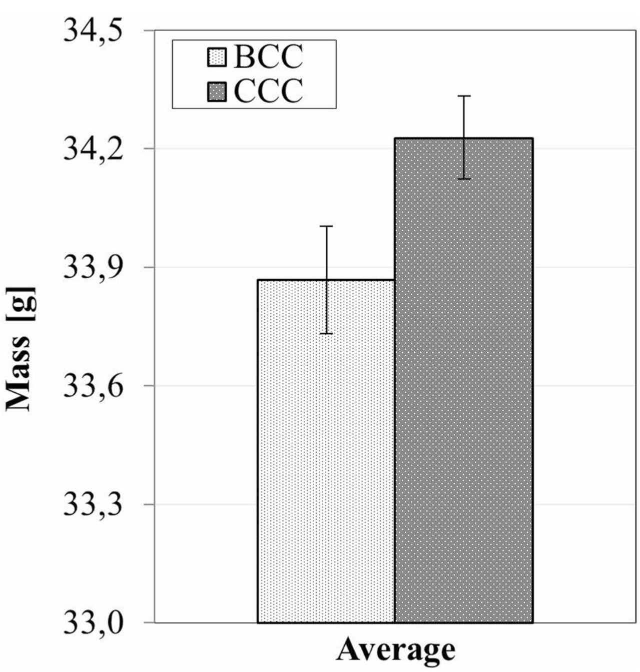

Fig. 12 Mass of the parts produced using BCC and CCC molds

For the Shapiro–Wilk test and the Mann–Whitney U test, statistical significance was evaluated at the 0.05 level, such that results with $p \leq 0.05$ were considered evidence against H_0.

In the mold with CCC, the SEM images revealed a thicker skin accompanied by a transitional layer between the shear region and the core, a feature absent in the mold with BCC. This transitional layer indicates that the thermal and shear gradients were more uniformly distributed across the specimen thickness (Fig. 11a and b), thereby smoothing the transition between the oriented skin and the crystalline core. Furthermore, the core exhibited smaller and more densely nucleated spherulites. Such a fine and compact microstructure minimizes irregular shrinkage and the formation of minor inter-spherulitic regions.

Therefore, the thicker skin, the presence of a transitional layer, and regions with minor inter-spherulitic variations might have contributed together to an increase in the density of parts molded using the CCC mold.

4 Conclusions

Based on the current literature, injection molds with conformal cooling channels (CCC) manufactured via metal additive manufacturing (Laser Powder Bed Fusion-LPBF) have demonstrated efficacy in reducing molding cycle time. However, for industrial applications, it is essential to understand how such a reduction in cycle time can affect the quality of the molded parts, yet the current literature lacks this information.

Thus, the present research was conducted to assess the quality of plastic parts produced by injection molding using a metal mold with CCC, manufactured via metal additive manufacturing (LPBF). To be closer to industrial application, a real automotive polypropylene component was used as the workpiece, and a set of injection molding experiments was conducted using a mold with a conventional baffle cooling channel (BCC) and a mold with CCC.

The CCC mold reduced the molding cycle time by 26%. Even that, the mass of the molded workpieces was heavier than the workpieces molded by the conventional mold (BCC), meeting an industrial quality indicator. The higher heat transfer rate and uniform shrinkage achieved by the CCC mold result in parts that are 83% more precise than those produced by the conventional mold (BCC). The CCC mold also reduces temperature gradients across the part, improving dimensional accuracy.

Compared with BCC, the samples produced by CCC mold increased the frozen, refined, and skin layers by about 53%, 6%, and 18%, respectively. Faster, more consistent cooling from the CCC mold increases skin thickness. This change is likely due to faster solidification at the surface, which promotes molecular alignment and density near the mold walls. These structural adjustments strengthen the outer regions of the part. Regarding the shear layer, a low cooling rate increases material ductility, making it easier to deform and flow during shear band formation and resulting in a thinner shear layer (3%) on BCC samples.

The BCC mold promotes the formation of larger and sparsely distributed spherulites. In contrast, CCC samples benefit from more efficient and uniform heat dissipation, which leads to smaller spherulites (47%) and a more even distribution, limiting crystal growth and enhancing nucleation.

The conventional analyses of tensile, impact, and crystallinity showed no alterations in the properties of parts produced using CCC molds. However, the dynamic mechanical analysis (DMA) revealed a subtle increase in stiffness in these parts. This was likely due to the thick skin layer on parts molded by the conformal cooling mold, as observed by the microscopy (SEM). Even so, this subtle increase in stiffness was not sufficient to alter the conventional analyses of mechanical properties.

The SEM images of samples produced by the CCC mold showed a transition region between the shear and core layers. As documented by Zhu et al. [30], the presence of a transition layer can increase the toughness of the plastic part, suggesting that CCC samples have greater potential for fracture toughness than those produced by the BCC mold, which showed only shear and core layers.

In industrial practice, the weight of parts furnished by a supplier is often used to ensure that they were produced within the specified cycle time. The results of the present work showed that parts produced by CCC molds were heavier, despite a shorter molding cycle time.

Then, conformal cooling can be applied to achieve greater stiffness and dimensional stability, especially at low deformations, without compromising toughness or strength. This is particularly desirable for parts operating in the elastic regime. Examples include automotive and household-appliance components such as interior panels, consoles, compartment covers, housings, and cabinets. These parts require dimensional stability, low warpage, and reduced vibration/noise. Stiffer skin improves structural integrity without requiring higher yield strength.

Given the great potential to reduce LPBF costs and the resulting trend toward increased use of molds with CCC, the results of this work corroborate this trend, showing that conformal cooling molds can be successfully used in industrial applications, reducing cycle time, improving geometric accuracy, and maintaining the mechanical properties of the molded parts.

Supplementary Information The online version contains supplementary material available at https://doi.org/10.1007/s00170-026-18276-2.

Author Contributions Alexandre Mateus Popiolek: Conceptualization, Methodology, Validation, Formal Analysis, Investigation, Data Curation, Writing – Draft, Writing – Editing, Visualization, Project administration, Funding Acquisition. Louis Laberge Lebel: Conceptualization, Funding Acquisition, Methodology, Project administration, Resources, Supervision, Validation, Writing – Editing. Carlos Henrique Ahrens: Methodology, Validation, Writing – Editing. Guilherme Barra: Methodology, Validation, Writing – Editing. Adriano Fagali de Souza: Conceptualization, Funding Acquisition, Methodology, Project administration, Resources, Supervision, Validation, Visualization, Writing – Editing.

Funding The Article Processing Charge (APC) for the publication of this research was funded by the Coordenação de Aperfeiçoamento de Pessoal de Nível Superior - Brasil (CAPES) (ROR identifier: 00x0ma614). This study has been supported by the Conselho Nacional de Desenvolvimento Científico e Tecnológico (CNPq) project 306438/2021-6 and doctorate scholarship (140898/2023-9), the Natural Sciences and Engineering Research Council (NSERC) of Canada, the Emerging Leaders in the Americas Program (ELAP) funded by the Government of Canada through Global Affairs Canada, Fundação de Amparo à Pesquisa e Inovação de Santa Catarina (Fapesc) project No. 2024TR002359, and also the company Branqs Automation and the BMW Group Brazil for their support on this research project.

Data Availability The data supporting this study's findings are available in the article and its supplementary information files, accessible at https://doi.org/10.5281/zenodo.18788744.

Declarations

Consent for publication All authors have read and agreed to the published version of the manuscript.

Competing interests No potential conflict of interest was reported by the author(s).

References

1. Kurt M, Kamber OS, Kaynak Y, Atakok G, Girit O (2009) Experimental investigation of plastic injection molding: Assessment of the effects of cavity pressure and mold temperature on the quality of the final products. Mater Des 30:3217–3224. https://doi.org/10.1016/j.matdes.2009.01.004

2. Park HS, Dang XP, Nguyen DS, Kumar S (2019) Design of advanced injection mold to increase cooling efficiency. Int J Precis Eng Manuf -Green Technol 7:319–328. https://doi.org/10.1007/s40684-019-00041-4
3. Shi F, Lou ZL, Zhang YQ, Lu JG (2003) Optimisation of plastic injection moulding process with soft computing. Int J Adv Manuf Technol 21:656–661. https://doi.org/10.1007/s00170-002-1374-3
4. Park HS, Dang XP (2017) Development of a smart plastic injection mold with conformal cooling channels. Procedia Manuf 10:48–59. https://doi.org/10.1016/j.promfg.2017.07.020
5. Park HS, Pham NH (2009) Design of conformal cooling channels for an automotive part. Int J Automot Technol 10:87–93. https://doi.org/10.1007/s12239-009-0011-7
6. Ovsik M, Fucikova K, Manas L, Stanek M (2024) Influence of polymer flow on polypropylene morphology, micro-mechanical, and tribological properties of injected part. Lubricants 12:202. https://doi.org/10.3390/lubricants12060202
7. Bociaga E, Kula M, Kwiatkowski K (2017) Analysis of structural changes in injection-molded parts due to cyclic loading. Adv Polym Technol 37:2134–2141. https://doi.org/10.1002/adv.21872
8. Kantz MR, Newman HD, Stigale FH (1972) The skin-core morphology and structure–property relationships in injection-molded polypropylene. J Appl Polym Sci 16:1249–1260. https://doi.org/10.1002/app.1972.070160516
9. Suksut B (2016) Morphology and morphology formation of injection molded PP-based nanocomposites. PhD Thesis, Technical University of Kaiserslautern, Germany
10. Varga J, Breining A, Ehrenstein GW, Bodor G (1999) Injection moulding of a commercial β-nucleated polypropylene. Int Polym Process 14:358–364. https://doi.org/10.3139/217.1545
11. Li J, Yang S, Turng L, Zheng W, Jiang S (2017) Comparative study of crystallization and lamellae orientation of isotactic polypropylene by rapid heat cycle molding and conventional injection molding. e-Polymers 17:71–81. https://doi.org/10.1515/epoly-2016-0251
12. Fischer J (2012) Handbook of Molded Part Shrinkage and Warpage, second edn. William Andrew, Oxford
13. Wright DGM, Dunk R, Bouvart D, Autran M (1988) The effect of crystallinity on the properties of injection moulded polypropylene and polyacetal. Polymer 29:793–796. https://doi.org/10.1016/0032-3861(88)90134-6
14. Fernandes ADC, de Souza AF, Howarth JLL (2016) Mechanical and dimensional characterisation of polypropylene injection moulded parts in epoxy resin/aluminium inserts for rapid tooling. Int J Mater Prod Technol 52:1–16. https://doi.org/10.1504/IJMPT.2016.073618
15. de Souza AF, Howarth JLL, Arendarchuck BE, Popiolek AM, Treml J, Kavilha C (2024) Alternative materials to shorten injection mold manufacturing and molding cycles. Polímeros 34:1–10. https://doi.org/10.1590/0104-1428.20230088
16. Park HS, Dang XP (2010) Optimization of conformal cooling channels with array of baffles for plastic injection mold. Int J Precis Eng Manuf 11:879–890. https://doi.org/10.1007/s12541-010-0107-z
17. Kumar S, Park HS, Lee CM (2020) Data-driven smart control of injection molding process. CIRP J Manuf Sci Technol 31:439–449. https://doi.org/10.1016/j.cirpj.2020.07.006
18. Shayfull Z, Sharif S, Mohd A, Zain M, Ghazali MF, Saad RM (2013) Potential of conformal cooling channels in rapid heat cycle molding: A review. Adv Polym Technol 33:1–24. https://doi.org/10.1002/adv.21381
19. Xu X, Sachs E, Allen S (2001) The design of conformal cooling channels in injection molding tooling. Polym Eng Sci 41:1265–1279. https://doi.org/10.1002/pen.10827
20. Marques S, de Souza AF, Miranda J, Yadroitsau I (2015) Design of conformal cooling for plastic injection moulding by heat transfer simulation. Polímeros 25:564–574. https://doi.org/10.1590/0104-1428.2047
21. Lu CT, Chen GS, Tseng SC (2017) Effectiveness of conformal cooling for a V-shaped plate and its influence on warpage. ICICE Proc 79–82. https://doi.org/10.1109/ICICE.2017.8479294
22. Park HS, Dang XP, Song XP (2017) Improving the cooling efficiency for the molding of a complex automotive plastic part by 3D printing technology. Trans Korean Soc Automot Eng 25:508–515. https://doi.org/10.7467/KSAE.2017.25.4.508
23. Singh D, Joshi K, Patil B (2022) Comparative economic analysis of injection-moulded component with conventional and conformal cooling channels. J Inst Eng 103:307–317. https://doi.org/10.1007/s40032-021-00778-5
24. Marin F, de Souza AF, Ahrens CH, de Lacalle LNL (2021) A new hybrid process combining machining and selective laser melting to manufacture an advanced concept of conformal cooling channels for plastic injection molds. Int J Adv Manuf Technol 113:1561–1576. https://doi.org/10.1007/s00170-021-06720-4
25. Marin F, de Souza AF, Mikowski A, Fontanella LHG, Soares P, de Lacalle LNL (2023) Energy density effect on the interface zone in parts manufactured by laser powder bed fusion on machined bases. Int J Precis Eng Manuf -Green Technol 10:905–923. https://doi.org/10.1007/s40684-022-00470-8
26. BASF (2025) Technical Information: Estimating Cooling Times in Injection Moulding. BASF Plastics, São Paulo
27. EMIC (2024) Manual: impact device for plastics. São José dos Pinhais
28. Popiolek AM, Lebel LL, Ahres C, Barra GMO, de Souza AF (2026) Mechanical properties of plastic parts produced by molds manufactured by additive manufacturing technology (LPBF) with conformal cooling channels – Supplementary material. https://doi.org/10.5281/zenodo.18788744. Zenodo
29. Grebowicz J, Lau S-F, Wunderlich B (1984) The thermal properties of polypropylene. J Polym Sci Polym Symp 71:19–37. https://doi.org/10.1002/polc.5070710106
30. Zhu L, Xu X, Wang F, Song N, Sheng J (2008) Characterisation of the thickness of transition layer and its relation to mechanical properties of polypropylene/poly(ethylene-co-octene) blends. Mater Sci Eng A 494:449–455. https://doi.org/10.1016/j.msea.2008.04.053